CO_2 Capture in Ionic Liquids Based on Amino Acid Anions With Protic Side Chains: a Computational Assessment of Kinetically Efficient Reaction Mechanisms

Stefano Onofri, Henry Adenusi, Andrea Le Donne, and Enrico Bodo*[a]

Absorption and capture of CO_2 directly from sources represents one of the major tools to reduce its emission in the troposphere. One of the possibilities is to incorporate CO_2 inside a liquid exploiting its propensity to react with amino groups to yield carbamic acid or carbamates. A particular class of ionic liquids, based on amino acids, appear to represent a possible efficient medium for CO_2 capture because, at difference with current industrial setups, they have the appeal of a biocompatible and environmentally benign solution. We have investigated, by means of highly accurate computations, the feasibility of the reaction that incorporates CO_2 in an amino acid anion with a protic side chain and ultimately transforms it into a carbamate derivative. Through an extensive exploration of the possible reaction mechanisms, we have found that different prototypes of amino acid anions present barrierless reaction mechanisms toward CO_2 absorption.

1. Introduction

The consequences of the increase in CO_2 emission by various human activities represent a serious threat for the ecosystem.[1] Since about 80% of CO_2 emissions come from fossil fuels[2] and specifically, 60% from power plants, a substantial research effort is devoted to find economic, environmentally friendly and efficient ways to capture and store CO_2 at the production sites.[3] Among others, some of the capture techniques are based on exploiting the chemical reaction of CO_2 with amines.[4] These technologies are expensive and generally non-ecofriendly.[5]

Ionic liquids (ILs) have been explored as a greener alternative to aqueous amines for CO_2 capture since the early years of the past decade.[6] The advantage of ILs over other solvents lie in their negligible vapor pressure and their peculiar composition which allows them to be tailored for a specific task.[7] The study of specific ionic liquids for CO_2 capture is, at the moment, a very active field of research and its development has been summarized in several papers.[8] CO_2 can be absorbed inside ILs exploiting both physisorption and chemisorption, the latter being more promising given that the efficiency of absorption is greater. Chemisorption of CO_2 in ILs is achieved by its reaction with amino groups and obviously require their molecular components to contain $-NH_2$ groups with which CO_2 can react to form carbamates and carbamic acids.[9]

Among the many variations of ILs specifically synthetized for CO_2 chemisorption, a positive balance between absorption capacity, cost and biocompatibility is represented by a class of ILs in which the anion is made by a deprotonated amino acid (AA) which is also the only $-NH_2$ containing specie. Within these compounds, absorption can occur to various extents depending on the physical conditions and on the IL molecular composition: absorption ranges from 0.5 mol of CO_2 per mol of IL (2:1 mechanism) up to 1 mol of CO_2 per 1 mol of IL (1:1 mechanism) and sometimes even higher molar fractions.[10] It is clear that this range of results implies the existence of different reaction mechanisms that are not yet fully understood. The general reaction scheme of amines with CO_2 is well known[11] and can be summarized as:

$$-NH_2 + CO_2 \longrightarrow -NHCO_2H$$

$$-NHCO_2H + -NH_2 \longrightarrow -NHCO_2^- + -NH_3^+$$

Whether the reaction proceeds with a 1:1 or 2:1 stoichiometry depends on what extent the second reaction takes place after the initial carbamic acid formation. Experimental measurements[12] indicates that the initial monomolecular reaction is the key process for absorption. The undesired 2:1 ratio can be avoided if bulky substituents on the amino group are used as shown in Ref. [11].

This reaction can be divided into two steps shown in Scheme 1: (1) a pre-reaction complex formation (which has zwitterionic character) and (2) a proton transfer (PT) to either carboxylate terminals. In principle the two tautomeric forms of the resulting product are in equilibrium (3), in practice, we will see that one form is often markedly more stable than the other and the final product is only one.

In principle, the PT step, in the bulk liquid, could take place within the same anion or between two different anions. Since the second option seems less likely to occur because of Coulombic repulsive interactions between anions, we shall focus exclusively on the mono-molecular mechanism.

[a] S. Onofri, Dr. H. Adenusi, Dr. A. Le Donne, Prof. E. Bodo
Department of Chemistry,
University of Rome "La Sapienza",
P. A. Moro 5, 00185, Rome, Italy
E-mail: enrico.bodo@uniroma1.it

Supporting information for this article is available on the WWW under https://doi.org/10.1002/open.202000275

© 2020 The Authors. Published by Wiley-VCH GmbH. This is an open access article under the terms of the Creative Commons Attribution Non-Commercial NoDerivs License, which permits use and distribution in any medium, provided the original work is properly cited, the use is non-commercial and no modifications or adaptations are made.

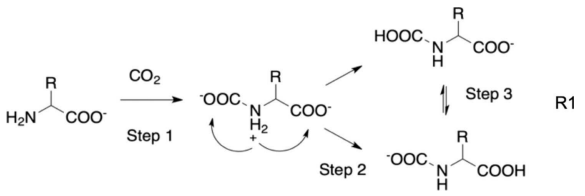

Scheme 1. The general reaction between an amino acid anion and CO_2. In the first step the zwitterionic pre-reaction complex is formed. An ensuing proton transfer (step 2) removes the zwitterion and forms either a carbamic acid derivative of its carbamate.

Several computational works have recently appeared in which various authors have explored the microscopic mechanisms that leads to the absorption stoichiometry detected in the experiments. Most of the theoretical efforts have been summarized in a recent review by Sheridan et al.[13] One of the most complete examinations of a variety of amino acid anions (mainly aliphatic ones) have been discussed in ref. [14] where the authors find that the rate limiting step in CO_2 chemisorption is the pre-reaction adduct formation and that, almost invariably, the ensuing carbamate formation reaction is exoergic. Shaikh et al. have studied the reaction mechanisms for $[Gly]^-$ coupled to various cations.[15,16] Both papers show the existence of barriers in the proton transfer step that leads the pre-reaction complex to the final carbamate. Mercy et al have investigated, among others, the reaction of the $[Ala]^-$ anion with CO_2[17] and they have found that the proton transfer step can occur via two possible reaction pathways that differ by the size of the ring that is formed in the transition state.

One of the major problems in using AA based ionic liquids is that they have high viscosities. This, in turn, reduces the diffusion process of CO_2 inside the liquid and makes the overall process inefficient. In addition, the ensuing liquid containing carbamate ions is generally more viscous than the original ionic liquid due to the increase in the number of hydrogen bonds.[18] The addition of water has been shown to significantly reduce the viscosity[19] and facilitate the reaction. In addition to decreasing the viscosity, water may act as a catalyst for the overall reaction[20] by driving a more efficient PT. In refs. [14,19] and [15], the authors have explored the role of a single water molecule on the kinetic of the PT and found that the inclusion of one water molecule effectively reduces some of the kinetic barriers of this step.

We feel that the computational data in the literature (at the moment of writing) are somewhat inhomogeneous and that the inevitable methodological differences between computation schemes do not always allow to univocally interpret the thermodynamics and kinetics of the reaction. We also feel that several possible reaction mechanisms due to the AA side chain might have been overlooked. We present here a systematic study of reaction **R1** using 3 prototypical different AA anions, two of which have protic and, possibly, active side chains: glycinate $[Gly]^-$, homocysteinate $[Hcys]^-$ and aspartate $[Asp]^-$. The reaction mechanism of the glycinate anion has been assessed before by calculations, but we have repeated the calculations here in order to provide a validation of the methods and models involved. The novelty of this paper lies in the calculations of the mechanisms for the two protic AAs which, as far as we know, have never been analyzed before and for which experimental determinations are still missing.

Following ref. [19], the general mechanisms of reaction R1 can be divided into three steps (see Scheme 1):

1. An initial pre-reaction complex formation whose efficiency is determined by the diffusion of CO_2 in the bulk liquid and by the energy necessary to "desolvate" the amino group and make it available for nucleophilic attack. The latter energy can be thought of as the energy required to break the ionic couple. The resulting pre-reaction complex is a zwitterionic anion and possess three separate charges: a positive one on the quaternary nitrogen and two negative ones on both CO_2 groups;
2. A PT from the ammonium group to the carboxylate groups to form a non-zwitterionic AA anion derivative (the primary product) with a carbamic acid group or a carbamate one, depending on which carboxylate is the proton acceptor. As we have mentioned above, the intramolecular PT pathway seems more likely to occur because anions do not come in close contact with each other owing to Coulomb repulsion;
3. Possibly, the formation of the primary product is followed by a fast tautomerization reaction (another PT) to form the other isomer, depending whether the latter structure is more stable.

In order to maintain the necessary generality, we had to simplify the overall problem by adopting a computational strategy which would render the results, as far as possible, independent of the many variables at play: (i) first of all, in the framework of high-quality ab-initio calculations, we are unable to account for the presence of an explicit bulk liquid. We try to take into account the effects of the liquid environment by using an approximate, but realistic, continuum solvent model. (ii) in all the calculations, we will not include a cationic partner. We do this mainly because we would like to maintain the widest generality and to focus exclusively on the reaction center. It is obvious that the cation does play a role in the reaction, however whether this role is an active one or that of a mere spectator, heavily depends on the cationic structure. It is very difficult to correctly address such role within the present calculation model, since the binding motif and strength of the ionic couple, when computed as an isolated system, turn out to be very different from those that one can find in the liquid. (iii) Since our aim is to provide information for reactions which actually take place in the liquid phase, we shall use energy differences instead of Gibb's free energy values (see the methods section for a detailed justification). (iv) The possible presence of water will be taken into account by considering only one explicit molecule as taking part in the reaction.

Computational Methods

The ab-initio calculations have been carried out for the reactants (**AR**, i.e. the isolated AA anion and CO_2 whose energy will be used as a reference throughout), for the pre-reaction complex (**CR**) and for the possible products (**P**). Since the formation of **CR** from **AR**

© 2020 The Authors. Published by Wiley-VCH GmbH

does not present any barrier, the only likely transition state (**TS**) has been localized between the pre-reaction complex **CR** and the products **P**. When the product **P** (which is necessarily similar to the transition state) presents a second tautomeric or isomeric structure with a lower energy, this has been explicitly computed and reported. For each structure, we have performed a fully unconstrained optimization and evaluated the harmonic frequencies using the dispersion-corrected B3LYP-D3 functional[21] with the 6-311+G(d,p) basis set. All minima and saddle points have been verified by computing the Hessian and by checking the relative vibrational frequencies. This combination is suitable for such a study since it provides results that are comparable to the more accurate CBS-QB3 and G4MP2 composite methods as we have verified for one of the reaction profiles (see SI, section S1). The Gaussian16[22] package was used for all the ab-initio calculations.

Given that some of these structures have charge separations (zwitterions) and can be substantially stabilized by a polar solvent, we have repeated all the stationary points calculations including an environmental dielectric screening via a continuum solvent model (PCM). Since the dielectric constant of these compounds is not known, we have adopted the acetonitrile PCM parameters as a realistic solvent model for its dielectric constant (35.7) matches the typical value of similar protic ILs.[23,24]

In each stationary point of the potential energy surface, the harmonic normal modes analysis provides us with a reliable approximation of the vibrational zero-point energy. We will therefore include it in all the energetic values reported in the rest of the paper. Also, the same analysis provides us with an estimate of the temperature dependent Gibbs free energy. Unfortunately, Gibb's free energy is evaluated using very approximate formulas (based on the perfect gas model) and is strictly valid only for gas-phase structures. Since our aim here is to provide information for a reaction taking place in the liquid, the approximations used for free energy evaluation would not be sufficiently correct and Gibb's free energy values might be misleading. For this reason, we will discuss our results reporting electronic energy differences (zero-point energy corrected) and we will report the corresponding free energies, for completeness, only in the SI.

2. Results and Discussion

2.1. Glycinate Anion

We begin by presenting our results for the $[Gly]^-$ anion. This is a small anion which provides the basic model for understanding the main reaction pathways and is here used as a validation of the computational approach. Reaction R1 proceeds in two steps, the former (formation of the zwitterionic adduct) has no barrier as it is expected for an ion-molecule reaction and is exoergic. The second step (the PT) can proceed via two different mechanisms: either the proton migrates onto the nearest carboxylate or onto the other one (see Scheme 2).

The two mechanisms differ by the number of atoms involved in the cyclic transition state. The PT to the nearest carboxylate (PT1-4) requires a 4-atoms ring transition state, while that to the farthest one (PT1-5) require a less strained 5-atoms ring.

The energy profile for the entire reaction R1 for the $[Gly]^-$ anion is given in Figure 1 and the corresponding structures are shown in Figure 2. The overall reaction profile (**AR**→**P2**) is

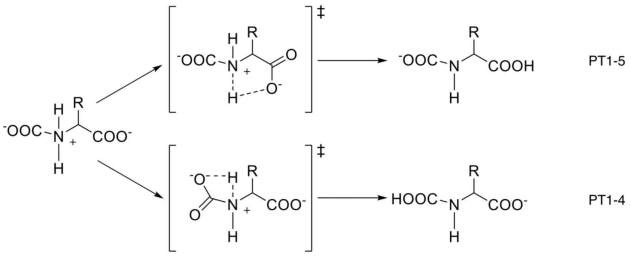

Scheme 2. Proton transfer mechanisms PT1-4 (bottom) and PT1-5 (top).

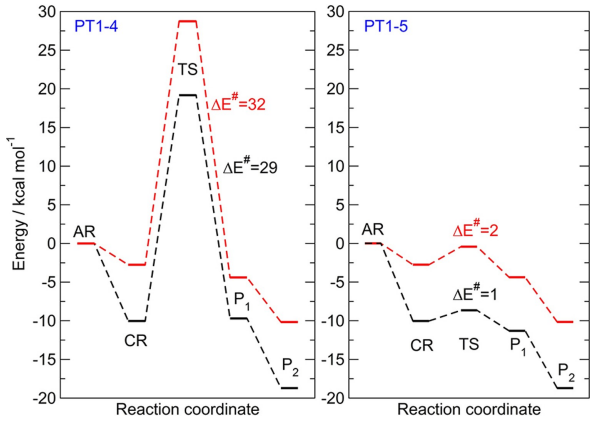

Figure 1. Energetic profile of reaction R1 for the $[Gly]^-$ anion. Left: the **PT1-4** path. Right: the **PT1-5** path. The transition state energies have been explicitly indicated in kcal/mol with respect to the pre-reaction complex CR.

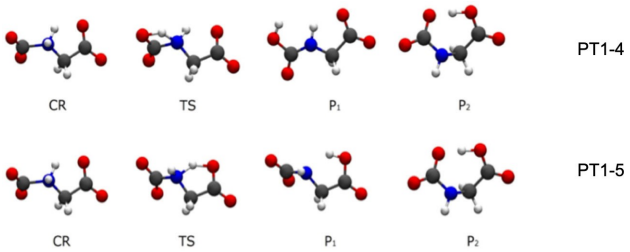

Figure 2. Rendering of the stationary points along the two reaction paths for $[Gly]^-$. For convenience only the gas-phase structures are shown.

exoergic of −19 and −10 kcal/mol for the calculation in vacuo and in PCM respectively. The first step that brings together the reactants in the pre-reaction complex (**AR**→**CR**) is barrierless and exoergic of −10 and −3 kcal/mol in vacuo and in PCM respectively. The reaction then proceeds by a PT (**CR**→**P1**) from the quaternary ammonium to the carboxylate and can undergo the two aforementioned mechanisms. The PT1-5 path presents a very low barrier in the PT step (~1–2 kcal/mol), while the PT1-4 path is hindered by a ~30 kcal/mol barrier. From the transition state, the nearest minimum is **P1** which is nearly isoergic with **CR** but it is not the most stable among the product structures. Internal rotation or an additional PT leads to the final lowest energy isomer **P2** (a carbamic acid).

The presence of a solvent medium (albeit in the form of an approximate model) tends to reduce the overall energy gain in the reaction. This is expected since the introduction of a solvent

© 2020 The Authors. Published by Wiley-VCH GmbH

model stabilizes the two isolated reactants (**AR**) structures more than all the others reaction intermediates due to the appearance of two solvation shells instead of only one. From the point of view of the pre-reaction complex (**CR**), however, the introduction of a model solvent does not change much the reaction profile with respect to the gas-phase results.

What we have just described agrees with what has been reported previously in the literature, albeit in slightly different setups (presence of the cation, absence of solvating continuum model, different methods and basis sets, etc.): in ref. [16], an analogous set of calculations has shown that the $[Ala]^-$ anion reaction proceeds with two PT mechanisms with barriers similar to ours; in ref. [15], a barrier of 3–4 kcal/mol was reported in the PT step (PT1-5) for the $[Gly]^-$ anion coupled to the $[P_{1111}]^+$ cation; in ref.[14] a barrier of ~30 kcal/mol was computed for the isolated $[Gly]^-$ anion when passing through PT1-4 path, a value which agrees with the present findings. In ref.[11] a derivative of the glycinate anion was used and the reaction enthalpy value reported therein (−10.4 kcal/mol) roughly agrees with what we find here (−11.4). Furthermore, the present mechanism agrees with that found in ref.[11] since both determinations show how the final preferred product of the reaction is a carbamic acid rather than a carbamate, a situation which tends to promote a 1:1 mechanism over the 2:1 one in agreement with experiments.

The relevant numerical data for the PT1-5 mechanism are summarized in Table S1.

2.2. Homocysteinate Anion

The second anion we have decided to study is $[Hcys]^-$ which, at difference with $[Gly]^-$, has the protic, weakly acidic group –SH on the side chain. In this case, PT can be achieved not only by involving the two carboxylate groups, but also the –SH terminal which, in the bulk phase, can exist also in its deprotonated form (thiolate).[25]

We begin by considering the possible reactive paths of an $[Hcys]^-$ anion where the carboxylate is deprotonated, and the proton is on the –SH group. For this tautomer, we have located the two PT1-4 and PT1-5 transition states which resembles the ones that we had found for $[Gly]^-$. They are not repeated here but shown in the SI in Figures S2 and S3. The barrier for PT1-4 for $[Hcys]^-$ is around ~30 kcal/mol and that for PT1-5 is ~2 kcal/mol both in vacuo and in model solvent. For the $[Hcys]^-$ anion, the most efficient mechanism is the one that transforms the initial anion in a carbamic acid derivative.

We know from previous calculations[26] that AA anions with protic side chains have tautomeric forms that are energetically competitive with the structures with a carboxylate. The tautomer of $[Hcys]^-$ with a COOH and an $-S^-$ group can also react with CO_2, but, given that the carboxyl group farthest from the CO_2 attack is already protonated, only a mechanism similar to PT1-4 is possible as shown in Scheme 3 on top. Such a mechanism (that we call PT2-4) has, as expected, a very high activation barrier of about ~30 kcal/mol in analogy with PT1-4 (see the SI, Figure S4).

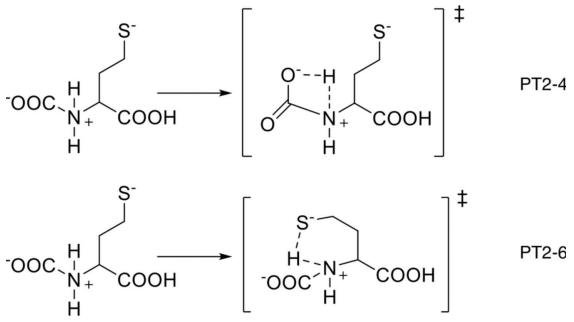

Scheme 3. Proton transfer mechanisms PT2-4 (top) and PT2-6 (bottom) in the reaction of an $[Hcys]^-$ anion and CO_2.

Another possibility (we call it **PT2-6**, Scheme 3 bottom) is that of having a PT to the S-group and, in this case, the structure passes through a very stable 6-atom ring which presents a negligible strain.

This reaction mechanism is shown in Figure 3 by reporting both its energetic profile and the stationary points structures. Mechanism **PT2-6** is a convenient one since it is globally exoergic of −28 kcal/mol and −18 kcal/mol in vacuo and PCM respectively. The activation barrier along this reaction path is non-existent.

It is clear that an AA anion with a sufficiently flexible protic side chain can present new reactive pathways to the carbamate formation and increase the kinetics of the reaction. The detailed data pertaining to the two most efficient mechanisms (PT1-5 and PT2-6) are reported in the SI in Table S2.

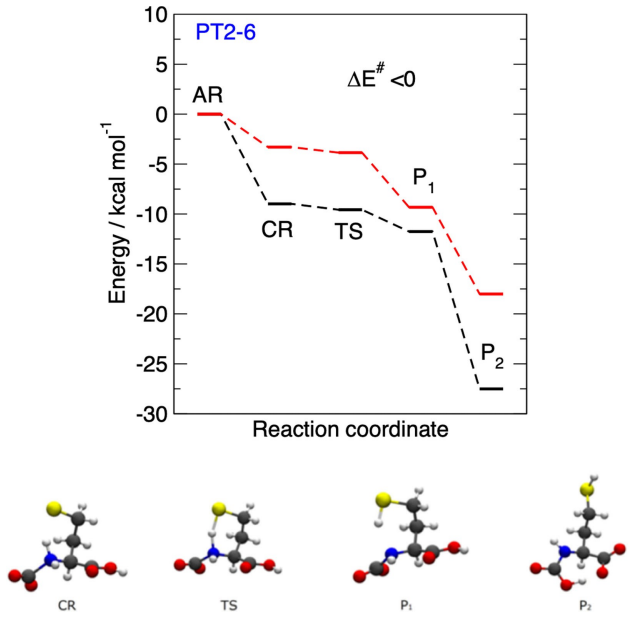

Figure 3. Top: Energetic profile of reaction R1 for the $[Hcys]^-$ anion following the PT2-6 mechanism. Black lines: in vacuo calculations. Red lines: PCM model solvent calculations. Bottom: rendering of the structures corresponding to the stationary points.

© 2020 The Authors. Published by Wiley-VCH GmbH

2.3. Aspartate Anion

Following the results for $[Hcys]^-$, we have analyzed $[Asp]^-$, an AA anion with a stronger acidic group on the side chain. In this case the acidity of the primary COOH group is comparable to the one on the side chain and both deprotonations are likely to occur in the liquid.

In order to make the exposition of the results clear, we will report here only those mechanisms that we have found to have a low-to-absent barrier to the PT. The first viable mechanism (Scheme 4, on top) is analogous to the PT1-5 found for $[Gly]^-$ and $[Hcys]^-$ and requires the formation, in the transition state, of a 5-atom ring for promoting the PT. The second mechanism is the analogue to PT2-6 of $[Hcys]^-$ and requires the deprotonation of the carboxyl on the side chains instead of the primary AA function (Scheme 4, bottom). Both energetic profiles are reported in Figure 4. Both mechanisms are exoergic, but surprisingly, and at difference with [Hcys], they present a considerable activation barrier.

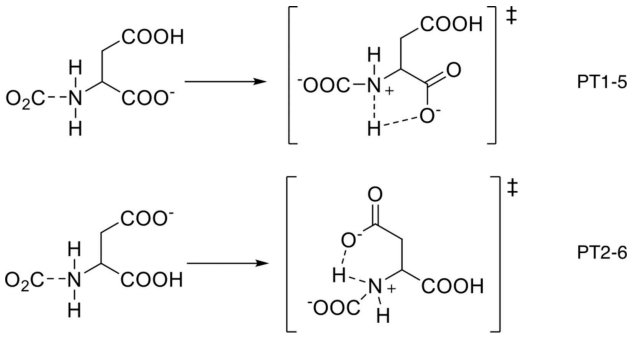

Scheme 4. Proton transfer mechanisms PT1-5 (top) and PT2-6 (bottom) in the reaction of an $[Asp]^-$ anion and CO_2.

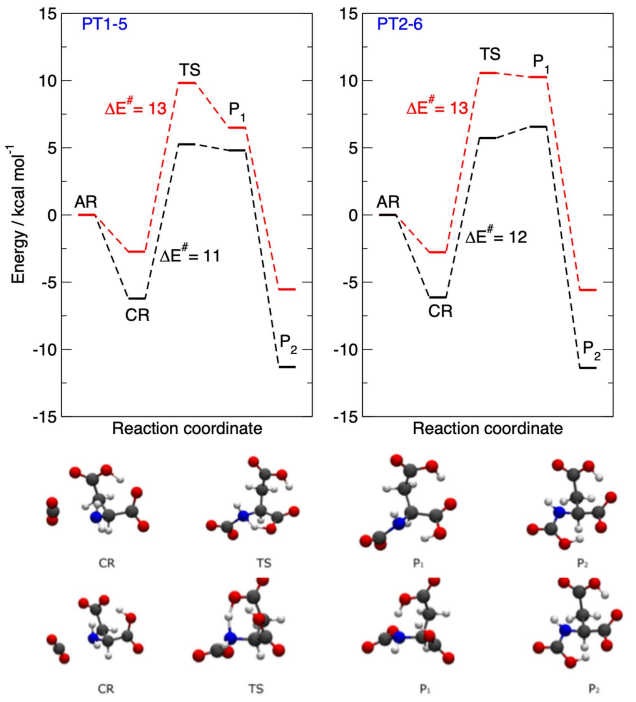

Figure 4. Top: energetic profile of reaction R1 for the $[Asp]^-$ anion following the PT1-5 (left) and PT2-6 (right) mechanism. Black lines: in vacuo calculations. Red lines: PCM model solvent calculations. Bottom: rendering of the structures corresponding to the stationary points for PT1-5 (top row) and PT2-6 (bottom row).

One of the peculiarities of the $[Asp]^-$ anion is that the bonding in the **CR** structure is less strong than in the previous reactions. The similarity of **CR** to **AR** produces an increase of the activation energies because the reaction now requires more energy for the formation of a viable transition state. This is due to the fact that, when in its isolated structure, the $[Asp]^-$ anion tend to form a very strong hydrogen bond between the two carboxyl groups and this reduces the propensity for CO_2 to attack the amino group. This should also be clear by looking at the **CR** structures in Figure 4 where the pre-reaction complex is characterized by a large distance between the CO_2 and the $-NH_2$ group, a distance which is much larger than those previously seen for $[Gly]^-$ or for $[Hcys]^-$.

The result is that, for $[Asp]^-$, the nucleophilic attack of CO_2 costs some energy and the transition states of both PT1-5 and PT2-6 are substantially higher than those found previously and turn out to be in both cases between 11 and 13 kcal/mol depending on the calculation conditions.

In addition, the $[Asp]^-$ reaction has to pass through a primary product $\mathbf{P_1}$ whose energy is competitive with the transition state and is much higher than the final structure $\mathbf{P_2}$ that is stabilized by two intramolecular hydrogen bonds. Although the conversion between $\mathbf{P_1}$ and $\mathbf{P_2}$ is a simple rearrangement of the molecular structure due to internal rotations, the relative instability of $\mathbf{P_1}$ could lead to a less efficient reaction pathway for $[Asp]^-$ if the conversion of $\mathbf{P_1}$ to $\mathbf{P_2}$ is not fast enough.

Therefore, the existence in $[Asp]^-$ of a strong intramolecular hydrogen bonds makes the reaction with CO_2 more difficult and kinetically much less efficient.

It turns out, however, that there exists a possible barrierless pathway to reaction R1 also for $[Asp]^-$. To achieve this, we have to assume that, initially, the $[Asp]^-$ anion does not contain the intramolecular hydrogen bond. In this case the propensity to react with CO_2 is similar to the one seen for $[Hcys]^-$. Such a mechanism (reported in Figure 5) is similar to PT2-6 already described for [Hcys]. It involves a 6-atoms cycle in the transition state and, since the energy of the reactants has increased upon breaking the intramolecular hydrogen bond, the reaction is barrierless and exoergic.

Overall, the presence of strong intramolecular hydrogen bonds in the target anion can hinder the reaction and reduce its efficiency. On the other hand, if the carboxylates are involved in intermolecular hydrogen bonds the reaction might proceed via more favorable energetic profiles. Using AA anions with longer side chains such as [Glu] may also reduce the tendency for tight internal hydrogen bonds and provide a more favorable reaction kinetic.

© 2020 The Authors. Published by Wiley-VCH GmbH

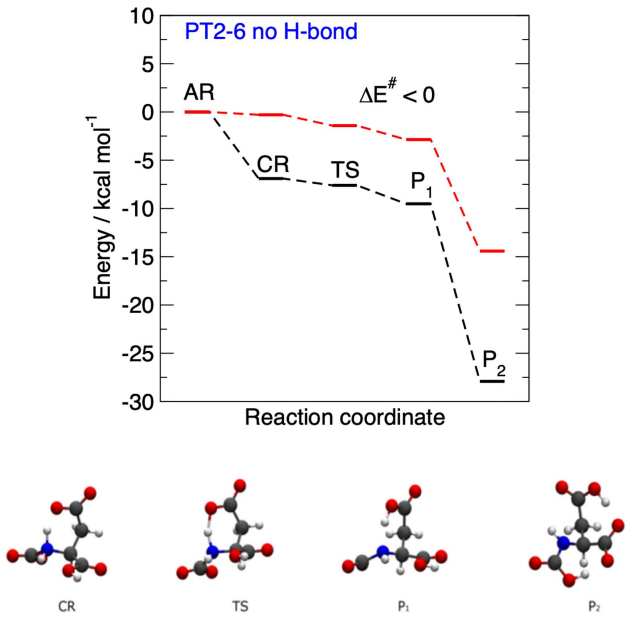

Figure 5. Top: Energetic profile of reaction R1 for the $[Asp]^-$ anion following the PT2-6 mechanism when no intramolecular H-bond is initially present in the anion. Black lines: in vacuo calculations. Red lines: PCM model solvent calculations. Bottom: rendering of the structures corresponding to the stationary points.

2.4. The Presence of Water

The addition of water to the initial IL, decreases its viscosity and makes the diffusion of CO_2 more efficient, thereby increasing the overall intake.[18] Water dissolves inside the ionic liquids and the resulting fluid microscopic structure can be very complex. For a clear (and necessarily simplified) interpretation, we make the assumption that only one water molecule partakes in the kinetically relevant step of the PT as shown in Scheme 5.

Our results indicate that, in all three AA anions, water can assist both the PT1-4 and the PT1-5 mechanisms by inserting itself inside the transition state ring. The addition of the water molecule to the 4-atoms cycle transition state (PTw-6) alleviates the strain by making it a 6-atoms cycle, thereby lowering significantly its kinetic barrier that changes from ~30 kcal/mol to less than 15 kcal/mol. On the other hand, the addition of a water molecule to the 5-atoms cycle transition state (PTw-7) causes a slight increase in its barrier by making a 7-atoms ring.

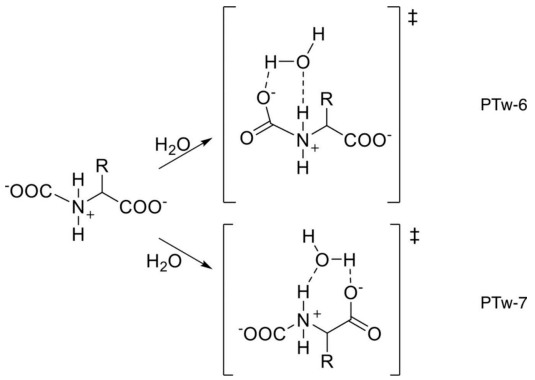

Scheme 5. Reaction mechanisms PTw-6 (top) and PTw-7 (bottom).

The prototypical energetic profiles and corresponding structures for the water-assisted mechanisms of $[Gly]^-$ are presented in Figure 6. The reaction, in the presence of water, remains exoergic with a gain of ~26 kcal/mol in the gas phase and of ~13 kcal/mol in the model solvent (see Table S3). Although the barriers of PTw-6 are much lower than those we had computed for PT1-4, this reaction mechanism continues to be kinetically inefficient with more than 10 kcal/mol of energy above **CR** (see ref.[19] for similar findings). On the other hand, even though the presence of water induces a slight increase of the kinetic barrier with respect to PT1-5, the PTw-7 mechanism remains viable at room temperature with a barrier of ~5 kcal/mol.

The two water-assisted mechanisms we have just seen for the $[Gly]^-$ anion are at play also for the two protic $[Hcys]^-$ and $[Asp]^-$ anions (they are reported in detail in Figures S5, S6 and S7). All mechanisms involving one water molecule for either [Hcys] or [Asp] are globally exoergic (see Table S5), but it becomes increasingly difficult to locate the lowest energy product for each reaction since its stability strongly depends on the position of the water molecule. The barriers for PTw-6 turns out to be ~13 kcal/mol and ~20 kcal/mol for [Hcys] and [Asp] respectively, still too high for the reaction to proceed efficiently through this channel. The barrier of PTw-7 is smaller and around 5–6 kcal/mol for [Hcys], while this mechanism remains inefficient for [Asp] where it costs more than 10 kcal/mol.

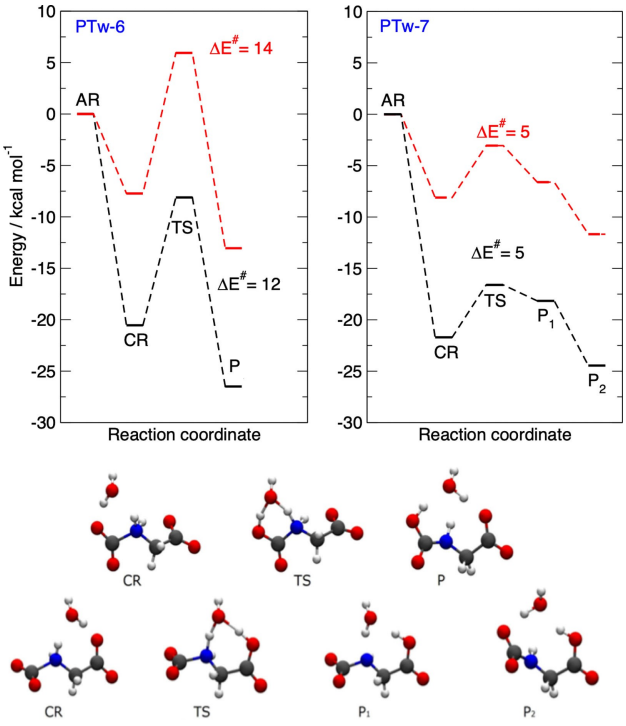

Figure 6. Top: Energetic profile of reaction R1 in the presence of water for the $[Gly]^-$ anion following the PTw-6 (left) and the PTw-7 (right) mechanism. Black lines: in vacuo calculations. Red lines: PCM model solvent calculations. Bottom: rendering of the stationary points structures in mechanisms PTw-6 (top row) and PTw-7 (bottom row).

© 2020 The Authors. Published by Wiley-VCH GmbH

The possible role of the side chains (once deprotonated) has also been explored and a possible additional reaction path involving an 8-atoms cycle (PTw-8) has been found for the $[Hcys]^-$ anion and is reported in Figure S5 and S6. This path has a barrier that seems to depend strongly on the presence of the model solvent and, due to its relatively low height (~5 kcal/mol), may represent a viable route to the products.

In conclusion, despite being all exoergic, most of the water-catalyzed mechanisms for the two protic AA anions are hindered by kinetic barriers above 10 kcal/mol. The only exceptions are the PTw-7 and PTw-8 transition states for $[Hcys]^-$ that present an energy which is only 5–6 kcal/mol above the **CR** complex (Figure S6) and thus still represents a viable mechanism for CO_2 absorption.

3. Conclusions

In this work we have explored through ab-initio computations the mechanisms of the reaction of three representative AA anions with CO_2. The reaction is characterized by a two-step mechanism where an initial nucleophilic attack leads to the formation of a zwitterionic complex which then evolves through a proton transfer to the product, i.e. a carbamate or a carbamic acid derivative of the original AA anion. Given the intrinsic limits of ab-initio computations we have not described the issues related to the gas diffusion inside the liquid, but we have only undertaken the study of the reaction once the CO_2 molecule is free to react with a nearby anion. Although bimolecular reactions are possible, in order to simplify the exploration of the many reaction mechanisms, we have limited this study to one anion only, and we have not taken into consideration intramolecular reactive pathways. Despite the relative simplicity stemming from the above assumptions, we have found that the possible reactive pathways, especially when considering AA anions with protic side chains, are various and some of them proceed without any activation barrier thereby providing a rough guide to choose potential candidates for an efficient absorption process.

The formation of the initial, stable, pre-reaction complex has been consistently found to be without barrier. Although this is certainly true for an isolated AA anion, it does not necessarily hold when the anion is strongly coordinated to a cation or is involved in intramolecular hydrogen bonds. The presence of these environmental effects, however, is out of the scope of the present research and will be assessed elsewhere. It is nevertheless true that once an AA anion is sufficiently near a CO_2 molecule the formation of the pre-reaction complex is fast and exoergic.

The ensuing evolution of the pre-reaction complex requires a proton transfer from the nitrogen to one of the carboxylates. Such a step, in general, appears hindered by kinetic barriers, but we have found it to be invariably exoergic, thus determining the overall addition reaction of CO_2 to an AA anion to be a globally exothermic process.

The proton transfer step can proceed via different mechanisms depending on the nature of the AA anions. Aliphatic AA (e.g. [Gly] and [Ala]) present two possible mechanisms, one of which (PT1-5) has a very low barrier and represent the main route to carbamate/carbamic acid formation inside these substances.

A protic side chain (e.g. [Hcys] and [Asp]) induces the presence of additional reaction channels. The presence of a weakly acidic side chain ([Hcys], mechanisms PT2-6) has been shown to provide a means to render the overall reaction more efficient by lowering the activation barrier of the proton transfer from 2–3 kcal/mol to none. A more acidic side chain ([Asp]) plays an analogous role, but it also induces tighter hydrogen bonding networks (intramolecular) and thus results in actually hindering the reaction site making the reaction far less efficient increasing the barriers up to ~10 kcal/mol. Breaking these hydrogen bonds restores the high efficiency of the overall process.

In this respect, the addition of water might promote a catalytic action inside the fluid. Actually, what we have found with our calculations is that, while water might be beneficial in lowering some of the activation barriers for the less efficient mechanisms, it generally causes a slight increase for the more efficient ones. In other words, while water plays a role as a general catalyst by reducing viscosity or hydrogen bonding (thus increasing the diffusion of CO_2 as well as partially removing phenomena that render the reaction site less available), it seemingly does not provide, at least judging from the present results, a direct beneficial effect on the kinetics of the monomolecular mechanisms.

Acknowledgements

This work received financial support from "La Sapienza" (grants n. RG1181643265D950 and RM11916B658EF0BA). All authors gratefully acknowledge the computational support of CINECA (grants IsC78_LLL-2 and IsC69_LLL).

Conflict of Interest

The authors declare no conflict of interest.

Keywords: CO_2 storage · ionic liquids · green solvents · computational chemistry · protic side chains

[1] Climate Change 2014: a) *Synthesis Report. Contribution of Working Groups I, II and III to the Fifth Assessment Report of the Intergovernmental Panel on Climate Change* (Eds.: Core Writing Team, R. K. Pachauri, L. A. Meyer), **2014**, IPCC, Geneva, Switzerland; b) N. H. Stern, *The Economics of Climate Change: The Stern Review*, Cambridge University Press Cambridge, **2007**; c) M. Meinshausen, N. Meinshausen, W. Hare, S. C. B. Raper, K. Frieler, R. Knutti, D. J. Frame, M. R. Allen, *Nature* **2009**, *458*, 1158.

[2] *IPCC special report on carbon dioxide capture and storage*, (Eds.: B. Metz, O. Davidson, H. de Coninck, M. Loos, L. Meyer), **2005**, Cambridge University Press, Cambridge.

[3] a) J. D. Figuero, T. Fout, S. Plasynski, H. McIlvried, R. D. Srivastava, *Int. J. Greenhouse Gas Control* **2008**, *2*, 9–20; b) H. Yang, Z. Xu, M. Fan, R. Gupta, R. B. Slimane, A. E. Bland, I. J. Wright, *Environ. Sci.* **2008**, *20*, 14–

© 2020 The Authors. Published by Wiley-VCH GmbH

27; c) N. MacDowell, N. Florin, A. Buchard, J. Hallett, A. Galindo, G. Jackson, C. S. Adjiman, C. K. Williams, N. Shah, P. Fennell, *Energy Environ. Sci.* **2010**, *3*, 1645–1669.
[4] a) G. T. Rochelle, *Science* **2009**, *325*, 1652–1654; b) C. H. Hsu, H. Chu, C. M. Cho, *J. Air Waste Manage. Assoc.* **2003**, *53*, 246–252.
[5] A. B. Rao, E. S. Rubin, *Environ. Sci. Technol.* **2002**, *36*, 4467–4475.
[6] C. Cadena, J. L. Anthony, J. K. Shah, T. I. Morrow, J. F. Brennecke, E. J. Maginn, *J. Am. Chem. Soc.* **2004**, *126*, 5300–5308.
[7] a) M. J. Earle, K. R. Seddon, *Pure Appl. Chem.* **2000**, 72, 1391–1398; b) J. F. Brennecke, E. J. Maginn, *AIChE J.* **2001**, 47, 2384–2389.
[8] a) X. Luo, C. Wang, *Curr. Opin. Green Sust. Chem.* **2017**, *3*, 33–38; b) J. F. Brennecke, B. E. Gurkan, *J. Phys. Chem. Lett.* **2010**, *1*, 3459–3464; c) J. Huang, T. Rüther, *Aust. J. Chem.* **2009**, *62*, 298–308; d) S. Babamohammadi, A. Shamiri, M. K. Aroua, *Rev. Chem. Eng.* **2015**, *31*, 383–412.
[9] a) E. D. Bates, R. D. Mayton, I. Ntai, J. H. Davis, *J. Am. Chem. Soc.* **2002**, *124*, 926–927; b) D. Camper, J. E. Bara, D. L. Gin, R. D. Noble, *Ind. Eng. Chem. Res.* **2008**, *47*, 8496–8498; c) J. Zhang, S. Zhang, K. Dong, Y. Zhang, Y. Shen, X. Lv, *X. Chem. - Eur. J.* **2006**, *12*, 4021–4026; d) B. E. Gurkan, J. C. de la Fuente, E. M. Mindrup, L. E. Ficke, B. F. Goodrich, E. A. Price, W. F. Schneider, J. F. Brennecke, *J. Am. Chem. Soc.* **2010**, *132*, 2116–2117; e) B. F. Goodrich, J. C. de la Fuente, B. E. Gurkan, D. J. Zadigian, E. A. Price, Y. Huang, J. F. Brennecke, *Ind. Eng. Chem. Res.*, **2011**, *50*, 111–118.
[10] a) B. E. Gurkan, J. C. de la Fuente, E. M. Mindrup, L. E. Ficke, B. F. Goodrich, E. A. Price, W. F. Schneider, J. F. Brennecke, *J. Am. Chem. Soc.* **2010**, *132*, 2116–2117; b) B. F. Goodrich, J. C. de la Fuente, B. E. Gurkan, Z. K. Lopez, E. A. Price, Y. Huang, J. F. Brennecke, *J. Phys. Chem. B* **2011**, *115*, 9140–9150; c) B. F. Goodrich, J. C. de la Fuente, B. E. Gurkan, D. J. Zadigian, E. A. Price, Y. Huang, J. F. Brennecke, *Ind. Eng. Chem. Res.* **2011**, *50*, 111–118; d) S. Saravanamurugan, A. J. Kunov-Kruse, R. Fehrmann, A. Riisager, *ChemSusChem*, **2014**, *7*, 897–902.
[11] A.-H. Liu, R. Ma, C. Song, Z.-Z. Yang, A. Yu, Y. Cai, L.-N. He, Y.-N. Zhao, B. Yu, Q.-W. Song, *Angew. Chem. Int. Ed.* **2012**, *51*, 11306–11310.
[12] Y. S. Sistla, A. Khanna, *Chem. Eng. J.* **2015**, *273*, 268–276.
[13] Q. R. Sheridan, W. F. Schneider, E. J. Maginn, *Chem. Rev.* **2018**, *118*, 5242–5260.
[14] D. S. Firaha, B. Kirchner, *ChemSusChem* **2016**, *9*, 1–10.
[15] A. R. Shaikh, H. Karkhanechi, E. Kamio, T. Yoshioka, H. Matsuyama, *J. Phys. Chem. C* **2016**, *120*, 49, 27734–27745.
[16] A. R. Shaikh, M. Ashraf, T. AlMayef, M. Chawla, A. Poater, L. Cavallo, *Chem. Phys. Lett.* **2020**, *745*, 137239.
[17] M. Mercy, N. H. de Leeuw, R. G. Bell, *Faraday Discuss.* **2016**, *192*, 479–492.
[18] M. Pan, Y. Zhao, X. Zeng, *J. Zou Ener. Fuels* **2018**, *32*, 5, 6130–6135.
[19] W. Li, S. Wen, L. Shen, Y. Zhang, C. Sun, S. Li, *Ener. Fuels* **2018**, *32*, 10, 10813–10821.
[20] M. A. Hussain, Y. Soujanya, G. N. Sastry, *Environ. Sci. Technol.* **2011**, *45*, 8582–8588.
[21] S. Grimme, J. Antony, S. Ehrlich, H. Krieg, *J. Chem. Phys.* **2010**, *132*, 154104.
[22] M. J. Frisch, G. W. Trucks, H. B. Schlegel, G. E. Scuseria, M. A. Robb, J. R. Cheeseman, G. Scalmani, V. Barone, G. A. Petersson, H. Nakatsuji, *et al. Gaussian 16*, revision B.01; Gaussian, Inc.: Wallingford, CT, **2016**.
[23] Z. Wojnarowska, M. Paluch, *J. Phys. Condens. Matter.* **2015**, *27*, 073202.
[24] E. L. Bennet, C. Song, Y. Huang, J. Xiao, *J. Mol. Liq.*, **2019**, *294*, 111571.
[25] A. Le Donne, H. Adenusi, F. Porcelli, E. Bodo, *J. Phys. Chem. B* **2019**, *123*, 26, 5568–5576.
[26] A. Le Donne, E. Bodo, *J. Mol. Liq.* **2018**, *249*, 1075–1082.

Manuscript received: September 15, 2020
Revised manuscript received: October 15, 2020

© 2020 The Authors. Published by Wiley-VCH GmbH